Supporting Information for

Design and Synthesis of Multifunctional Gold Nanoparticles Bearing Tumor-Associated Glycopeptide Antigens as Potential Cancer Vaccines

Raymond P. Brinas[1], Andreas Sundgren[2], Padmini Sahoo[3], Susan Morey[3], Kate Rittenhouse-Olson[3], Greg E. Wilding[4], Wei Deng[4] and Joseph J Barchi Jr. [1]*

[1]Chemical Biology Laboratory, Center for Cancer Research, National Cancer Institute, Frederick National Laboratory for Cancer Research, Frederick, MD 21702, [2]Norwegian Medicines Agency Sven Oftedals vei 8, N-0950 Oslo, Norway, [3]Department of Biotechnical and Clinical Laboratory Sciences, University of Buffalo, Buffalo NY, 14214 and Department of Biostatistics, School of Public Health and Health Professions, University of Buffalo, Buffalo NY, 14214

Figures S1-S8: ^{1}H NMR spectra of synthetic intermediates and GNP's

Figures S9- S15 and Tables S1-S6: DLS data for vaccine constructs A-F

Figure S16: UV-vis spectra for vaccine constructs A-F

Figure S17 (Parts 1 and 2): TEM data for vaccine constructs A-F

Table S7: Size and CV table for vaccine constructs A-F

Figure S18: Zeta potential graphs for particles A-F

^{1}H NMR spectra of the thiol-terminated peptides/glycopeptides:

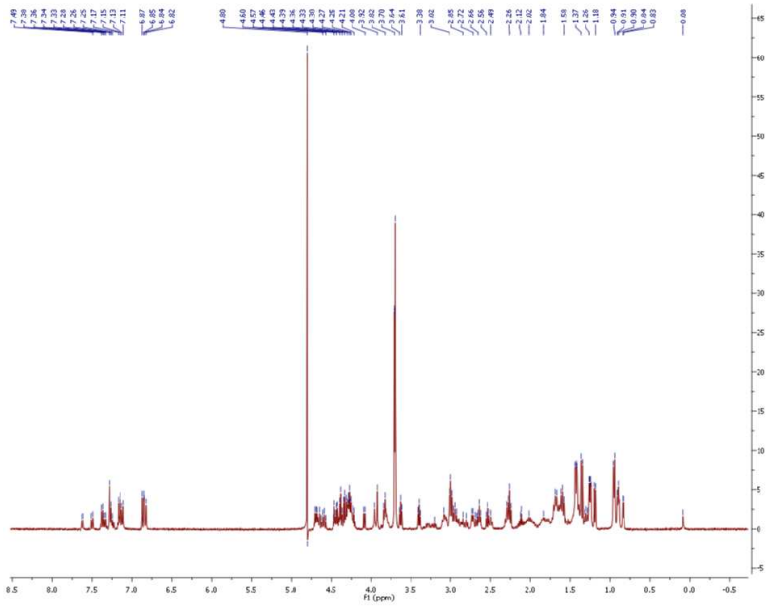

Figure S1. ^{1}H NMR spectrum of HS-Linker-KFLTTAKDKQRWEDPGKQLYQVEA-TSYA (**C3d**)

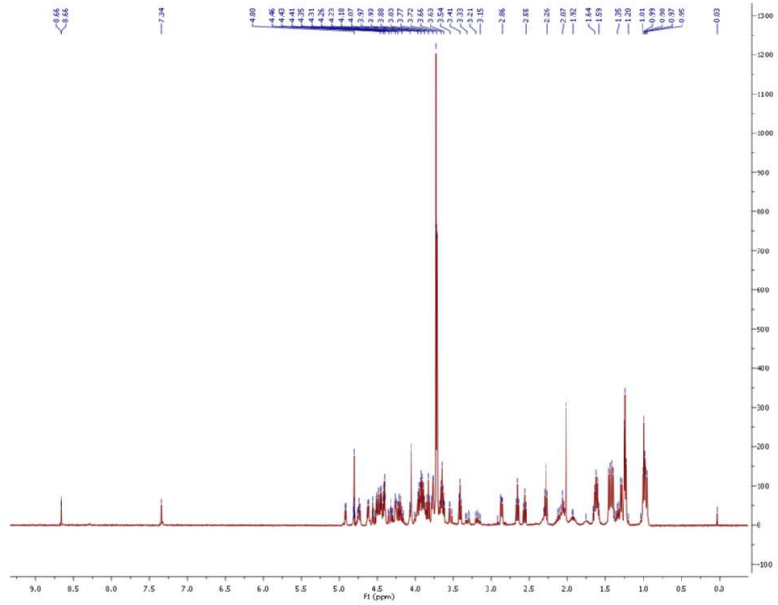

Figure S2. ^{1}H NMR spectrum of HS-Linker-TSSAS(Galβ1→3GalNAcα)TGHAT-PLPVTD **(5-TF)**

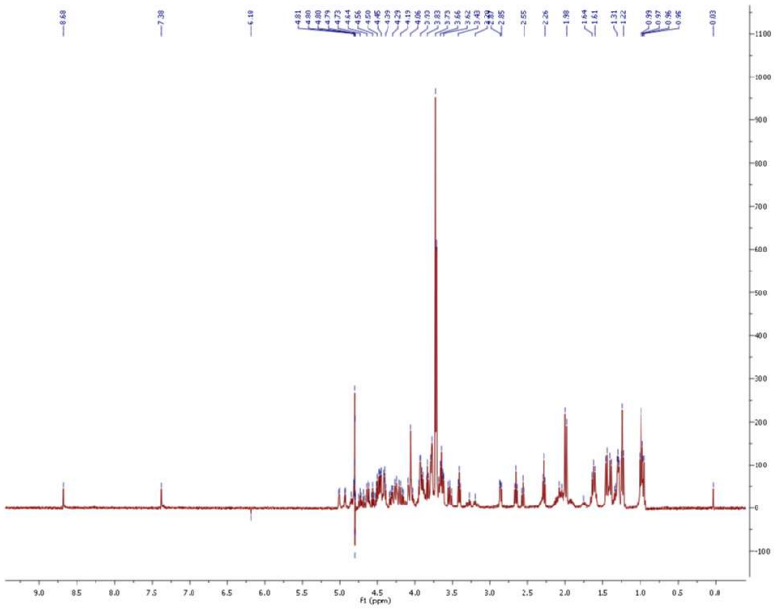

Figure S3. ^{1}H NMR spectrum of HS-Linker-TSSAS(Galβ1→3GalNAcα)T-(Galβ1→3GalNAcα)GHATPLPVTD **(5,6-TF)**

^{1}H NMR Spectra of the Vaccine Constructs:

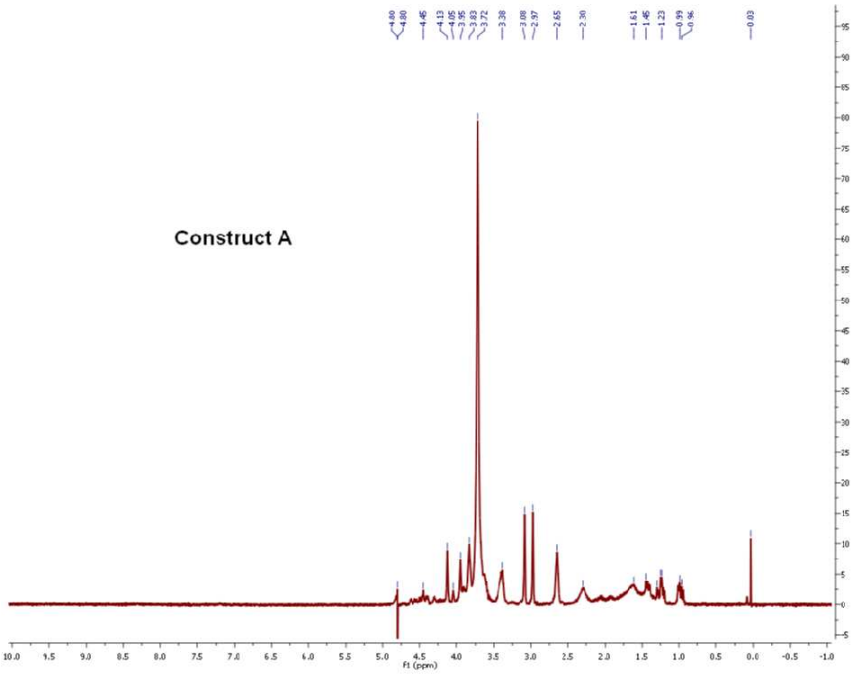

Figure S4. ^{1}H NMR spectrum of vaccine construct A.

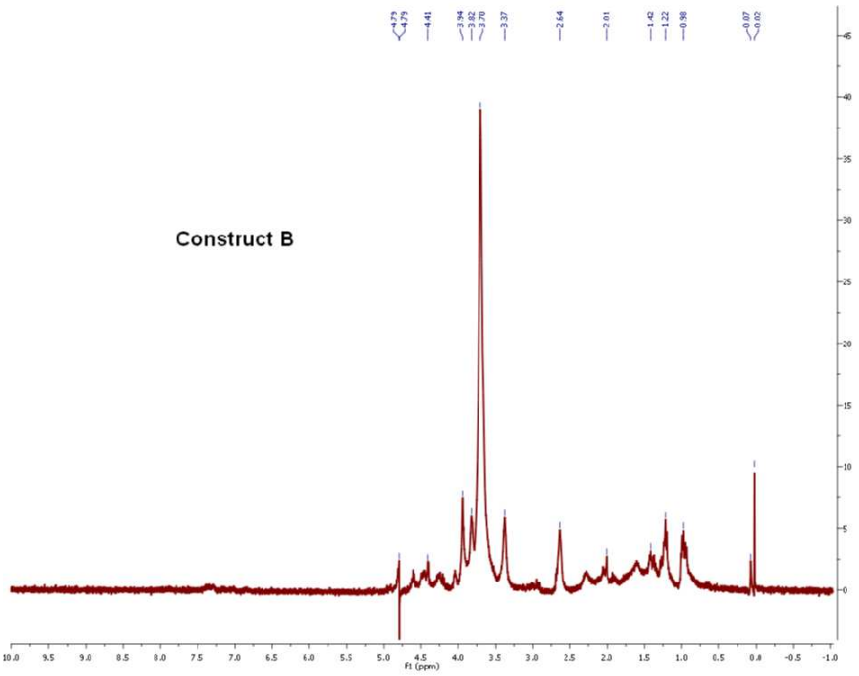

Figure S5. ^{1}H NMR spectrum of vaccine construct B.

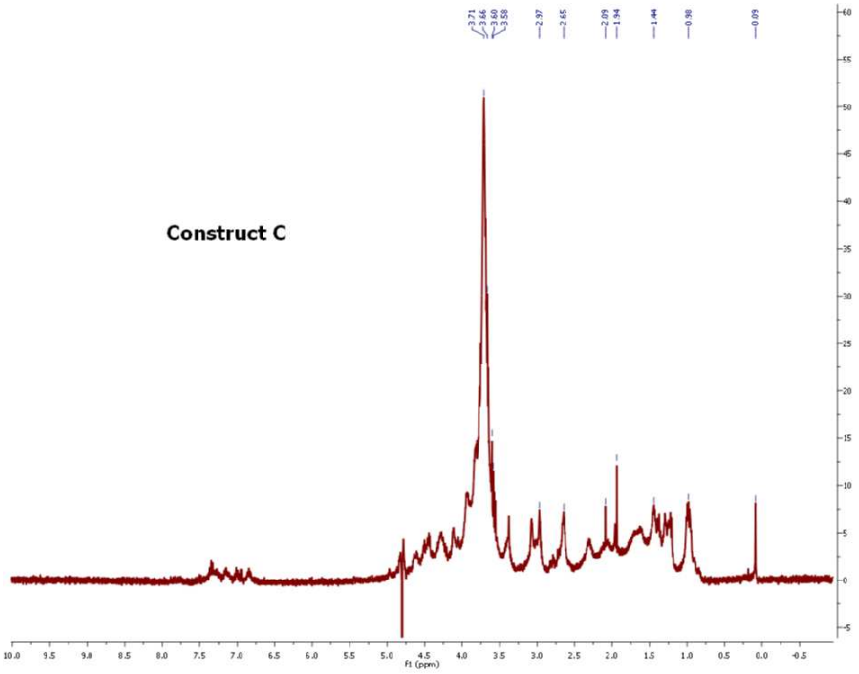

Figure S6. ^{1}H NMR spectrum of vaccine construct C.

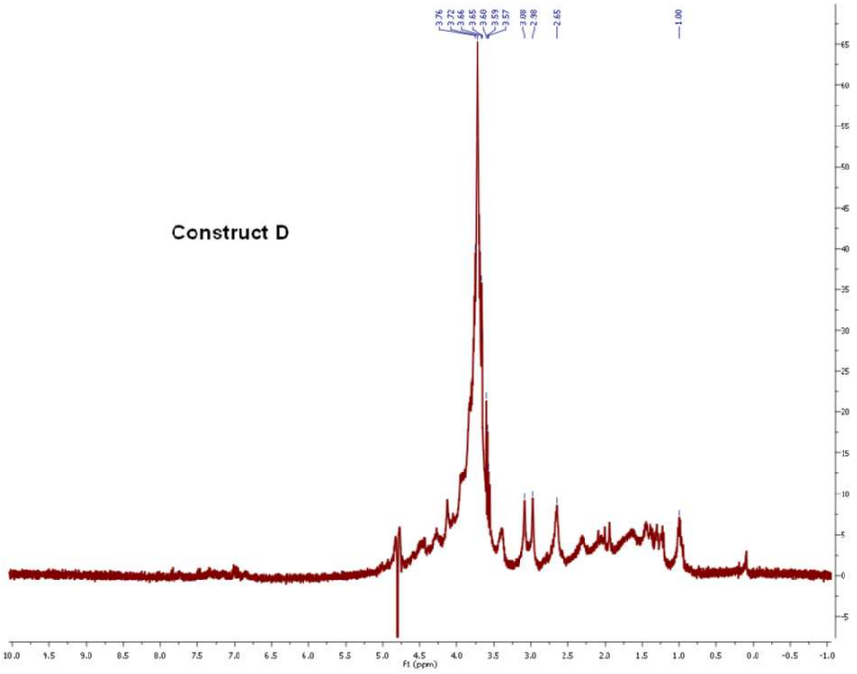

Figure S7. ^{1}H NMR spectrum of vaccine construct D.

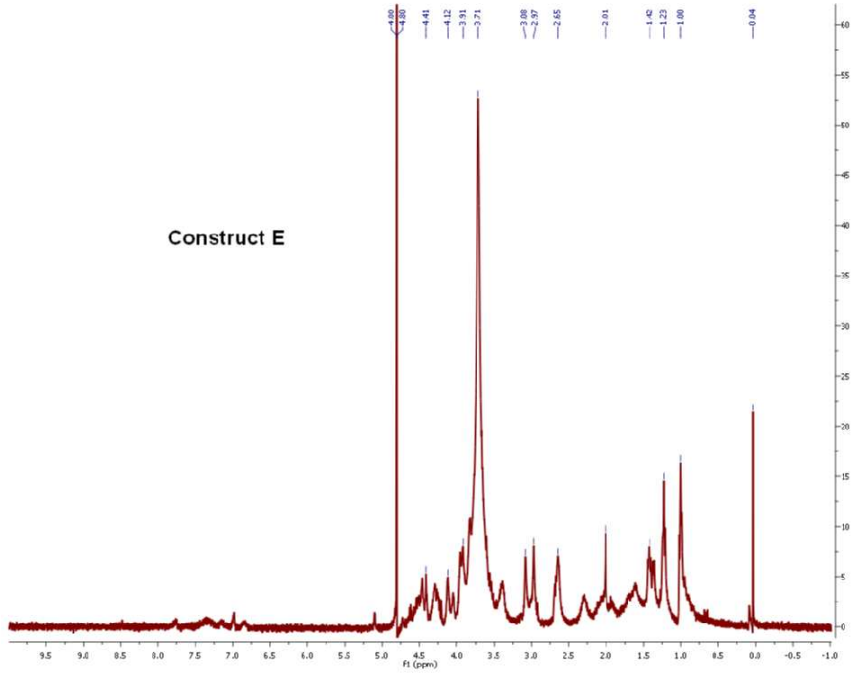

Figure S8. ^{1}H NMR spectrum of vaccine construct E.

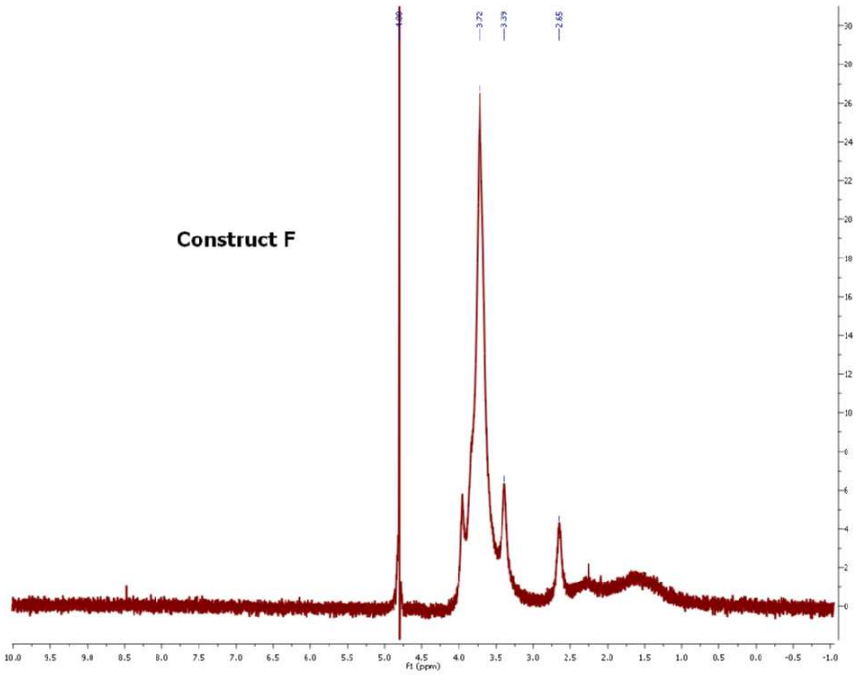

Figure S9. ^{1}H NMR spectrum of vaccine construct F.

Dynamic light scattering (DLS) data for the vaccine constructs:

Table S1. DLS data for construct A

Peak	Radius	% Polydispersity	% Mass
1	3.29	21.2	99.83
2	24.3	16.5	0.17

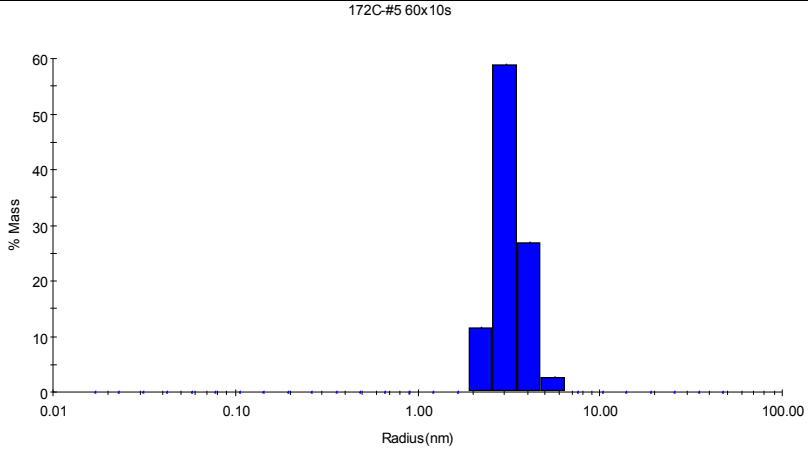

Figure S10. DLS size distribution of construct A

Table S2. DLS data for construct B

Peak	Radius	% Polydispersity	% Mass
1	2.933	22.0	99.87
2	23.569	18.1	0.13

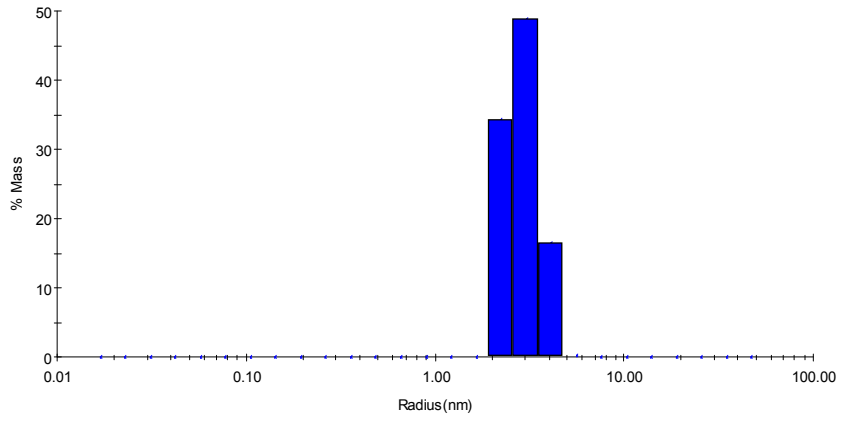

Figure S11. DLS size distribution of construct B

Table S3. DLS data for construct C

Peak	Radius	% Polydispersity	% Mass
1	2.914	41.3	99.89
2	29.845	24.7	0.11

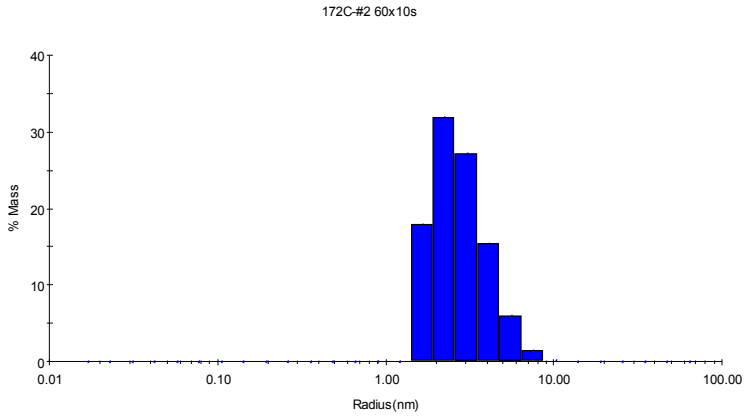

Figure S12. DLS size distribution of construct C

Table S4. DLS data for construct D

Peak	Radius	% Polydispersity	% Mass
1	3.390	55.2	100.00

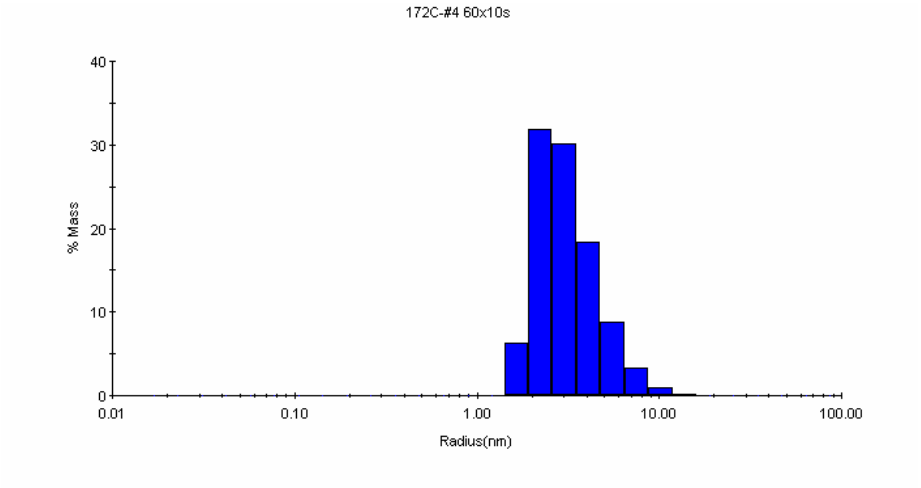

Figure S13. DLS size distribution of construct D

Table S5. DLS data for construct E

Peak	Radius	% Polydispersity	% Mass
1	5.164	32.1	99.81
2	33.076	24.8	0.19

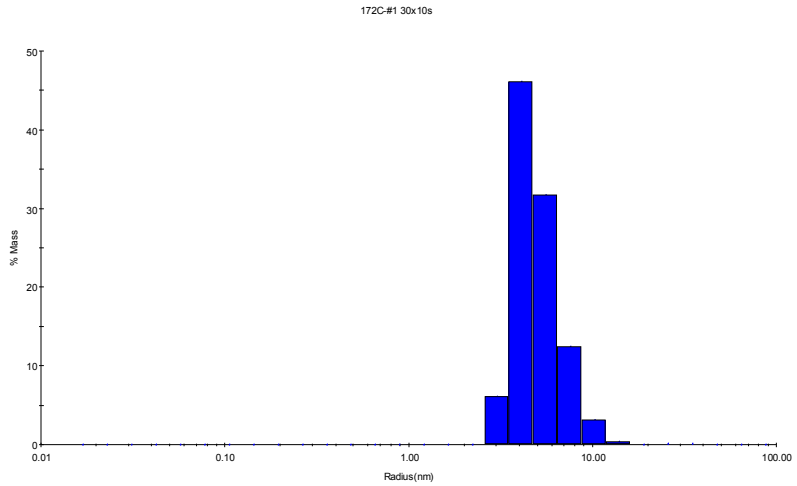

Figure S14. DLS size distribution of construct E

Table S6. DLS data for construct F

Peak	Radius	% Polydispersity	% Mass
1	3.300	39.5	100.00

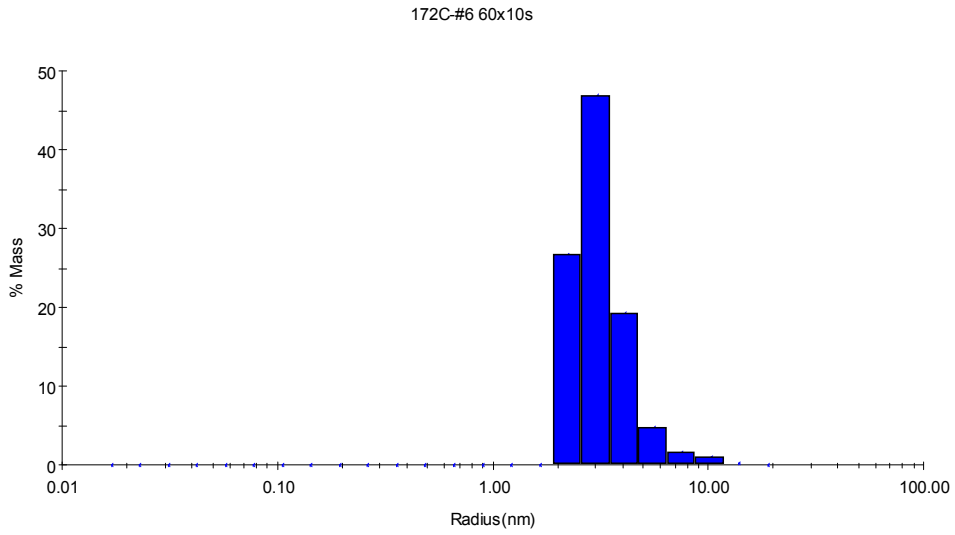

Figure S15. DLS size distribution of construct E

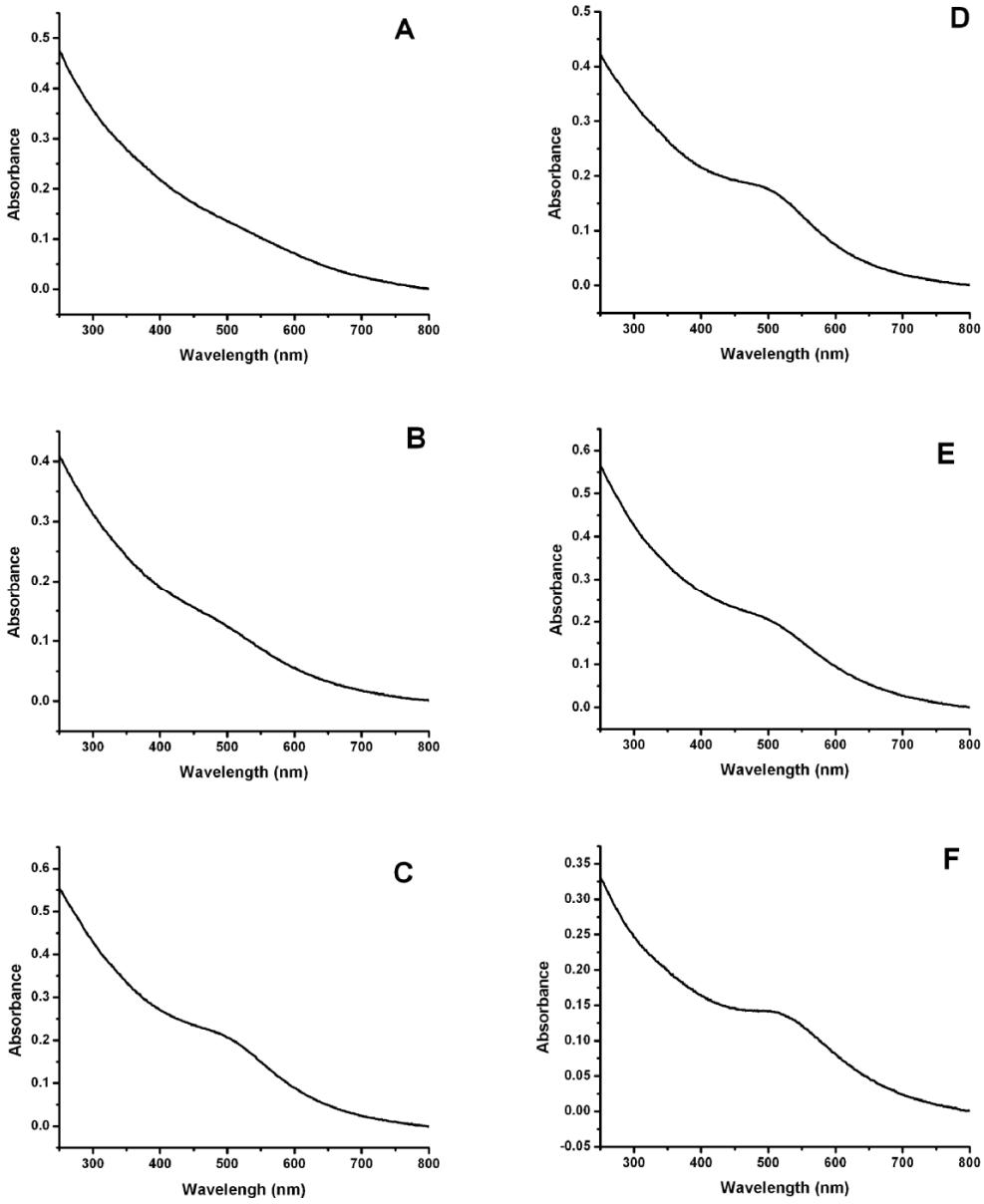

Figure S16. UV-Vis spectra of the vaccine constructs A-F

Transmission Electron Microscopy data for the vaccine constructs:

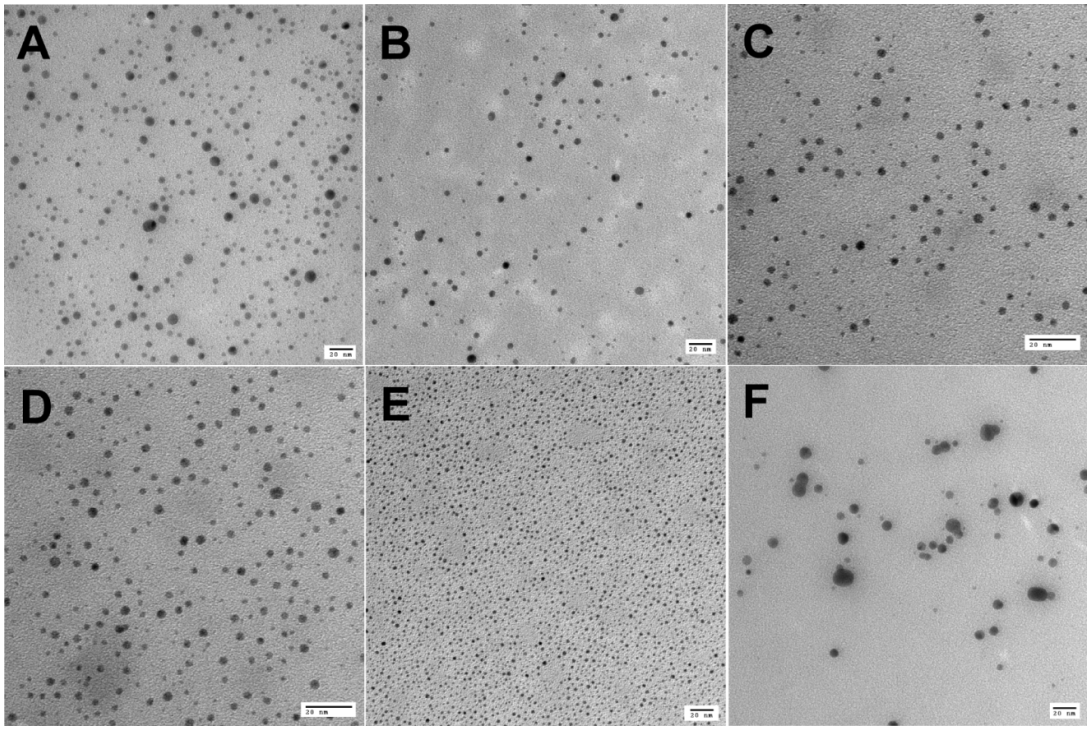

Figure S17. Part 1. TEM images of constructs A-F. The scale bars are all 20 nm.

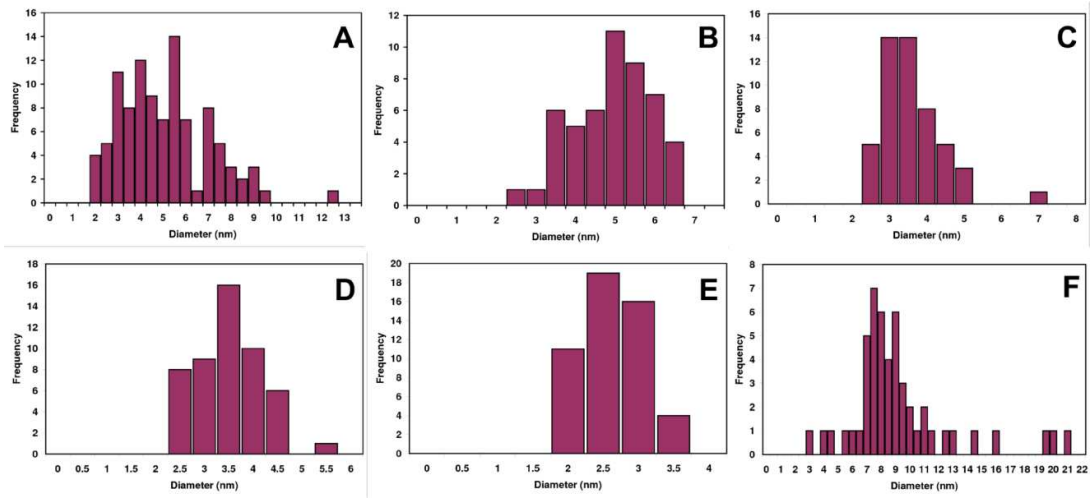

Figure S17. Part 2. TEM size distribution of constructs A-F

Table S7. TEM Analysis of the core size of the vaccine constructs

Construct	Mean size (nm)	Standard deviation (nm)	Coefficient of Variation (%)
A	4.82	2.03	42
B	4.70	1.00	21
C	3.35	0.76	22.7
D	3.28	0.67	20.4
E	2.40	0.45	18.8
F	9.02	3.61	40

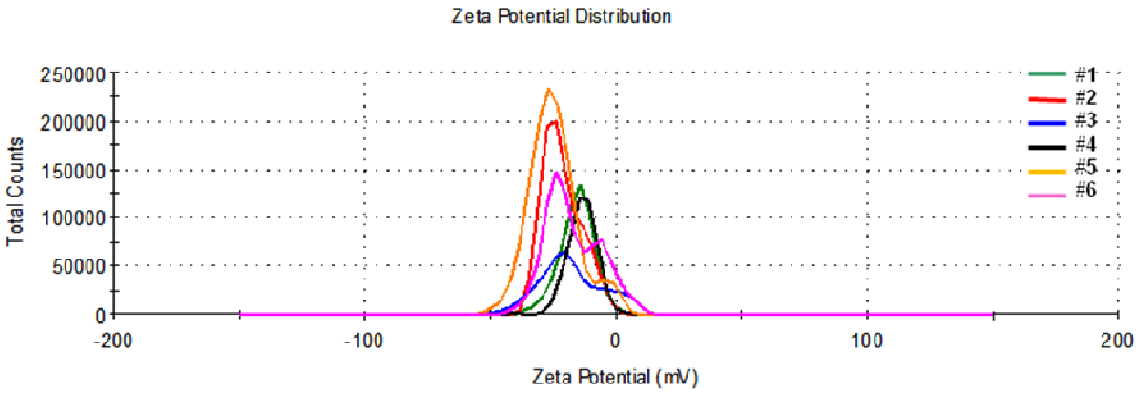

Figure S18. Zeta potential provides a measure of the electrostatic potential at the surface of the electrical double layer and the bulk medium, which is related to its surface charge. A Malvern Zetasizer Nano ZS instrument was used to measure zeta potential at 25° C for all samples. Stock samples were diluted 10-fold in 10 mM NaCl and loaded into pre-rinsed folded capillary cell for the zeta potential measurements. Sample pH was measured before zeta potential measurements. An applied voltage of 150 V was used. A minimum of three measurements were made per sample. Traces in the figures represent the average of the three measurements. Zeta potential measurements are based on first principles and hence no calibration is required. However, the instrument can be validated by running an appropriate standard (Zeta Potential Transfer Standard, DTS0050, zeta potential value of -50 ± 5 mV at 25 °C, Malvern Instruments). This standard was run before all zeta potential measurements for validation.